Materials and Structures (2022) 55:133
https://doi.org/10.1617/s11527-022-01981-1

ORIGINAL ARTICLE

Influence of selected reactive oxygen species on the long-term aging of bitumen

Kristina Hofer · Johannes Mirwald · Daniel Maschauer · Hinrich Grothe · Bernhard Hofko

Received: 23 February 2022 / Accepted: 4 May 2022 / Published online: 17 May 2022

Abstract The aging of bitumen is a major contributor to the failure of asphalt pavements. Realistic and accurate laboratory aging methods can predict bitumen durability and guarantee the use of high-quality components in asphalt pavement. However, current standardized aging methods do not incorporate atmospheric parameters, besides elevated temperatures and molecular oxygen. Crucial chemical components like reactive oxygen species (ROS), e.g. nitrogen oxides (NO_x) or ozone (O_3), are completely neglected. This study focusses particularly on the reactivity of individual ROS, such as nitrogen monoxide (NO), nitrogen dioxide (NO_2) and O_3, in regards to the long-term aging (LTA) of three unmodified bitumen. For LTA an adapted version of the Viennese Binder Aging method was used and the aged bitumen samples were analyzed with the dynamic shear rheometer and Fourier-Transform-Infrared spectroscopy, respectively. The results show that NO as a single component does not induce significant aging, whereas NO_2 leads to severe bitumen deterioration, which is even more accelerated when a second oxygen source is present. In comparison, the reactivity of O_3 is rather mild and it did not cause additional aging for two of the investigated binders. This study provides evidence, that ROS play a crucial role in bitumen aging and should thus not be neglected when addressing realistic aging conditions in the laboratory.

Keywords Bitumen · Long-term aging · Reactive oxygen species · DSR · FTIR

K. Hofer (✉) · J. Mirwald · B. Hofko
Christian Doppler Laboratory for Chemo-Mechanical Analysis of Bituminous Materials, Institute of Transportation, TU Wien, Karlsplatz 13/230-3, 1040 Vienna, Austria
e-mail: kristina.hofer@tuwien.ac.at

D. Maschauer
Institute of Transportation, TU Wien, Karlsplatz 13/230-3, 1040 Vienna, Austria

H. Grothe
Christian Doppler Laboratory for Chemo-Mechanical Analysis of Bituminous Materials, Institute of Materials Chemistry TU Wien, Getreidemarkt 9/E-165-01-5, 1060 Vienna, Austria

1 Introduction

Bitumen is a black, organic, visco-elastic material, that is refined from crude-oil via vacuum distillation [1]. Due to its unique adhesive and sealing properties it has been used by humanity for construction, waterproofing and for medical purposes for thousands of years [2–4]. Nowadays around 85% of all bitumen is used as a binder in asphalt mixtures and the remaining 15% are used in other applications, for instance as a sealing material in the roofing industry or in hydraulic engineering [1, 5]. Primarily, it consists of hydrocarbons and small amounts of oxygen, nitrogen and

sulfur, which makes it an organic material [6]. Hence, contact of bitumen with oxygen leads to aging, causing the material to become stiffer, more brittle and susceptible to cracking over time [7].

Bitumen aging is typically described by two processes and simulated separately:

(1) Short-term aging (STA) of bitumen occurs during construction and production caused by high temperatures and exposure to air. This process is simulated in the laboratory with the Rolling Thin Film Oven Test (RTFOT) [8].
(2) Long-term ageing (LTA) occurs during the service-life of bitumen and is caused by a variety of environmental phenomena, such as elevated temperatures, light, moisture and O_2 and reactive oxygen species (ROS) in the atmosphere. LTA is simulated in the laboratory with the Pressure Aging Vessel (PAV) [9]. During PAV aging a high temperature and pressure is applied to accelerate the aging process and to induce strong oxidation over a short period of time.

However, important aging inducing factors of the environment (moisture, light and ROS) have not been taken into account and are therefore not incorporated in the standardized laboratory long-term aging methods. Several studies have already reported an effect of moisture and light on bitumen and asphalt aging. First of all, water in combination with mechanical stresses can cause the loss of strength and durability, leading to debonding of the binder and the aggregate and adhesive or cohesive failure [10–13]. Furthermore, the interaction of bitumen with aqueous solutions of NaCl and Na_2SO_4 can change the surface roughness of asphalt mixtures and accelerates the erosion process according to Zou et al. [14]. Additionally, the effect of moisture damage coupled with oxidative aging has been addressed in literature using mostly a theoretical approach. Ma et al. state that the chemical structure and composition, viscosity and morphology are some of the important factors influencing the behavior towards aging induced by water and oxygen [15]. Das et al. show indications for the formation of water soluble thin films due to aging [16]. Albeit, there have also been studies indicating that water has very little influence on bitumen and asphalt aging [17] or that the influence of moisture varies among different bitumen samples [18], which underlines the need for further research concerning the impact of water.

A similar picture is shown regarding studies focusing on the effect of light on bitumen aging. There is a general agreement in literature that different wavelengths induce different degrees of aging [19, 20], but the mechanisms behind this phenomenon have not yet been fully uncovered. Light in the energy-rich UV range certainly has a severe impact on bitumen aging, but according to recent studies of Mirwald et al. also light at longer wavelengths, i.e. in the visible region, has a strong aging potential [21, 22]. Feng et al. have separated bitumen into the SARA fractions and have shown that the fractions on their own are more prone to UV-aging than the unseparated, original bitumen. Especially the saturates display the most changes after exposure to UV light [23]. Furthermore, the effect of ultraviolet absorbers (UVA) has been studied to a certain degree in various experimental setups. It is reported that UVAs can improve the UV aging and also the thermal-oxidative aging resistance [24], but the effect is strongly influenced by additional modifiers (e.g. polymers) [25, 26].

The third aforementioned parameter, that has mostly been disregarded when looking at bitumen aging in the past, is the influence of the atmosphere and therein occurring reactive oxygen species like ozone (O_3) and nitrogen oxides (NO_x). Ozone is formed in the atmosphere due to oxidation of hydrocarbons and carbon monoxide (CO) [27] and NO_x are emitted from car engines [28] in close proximity to asphalt pavements in the traffic system. The number of literature references on the effect of realistic aging conditions (including ROS) on bitumen or on other related materials is very limited and scattered, however an attempt is being made to give a cohesive picture of the so far available data. The influence of SO_2 and NO_x in combination with moisture on polymeric films was examined by Pagnin et al. [29]. The impact of the different gas species varied between the investigated films, whereby NO_x caused more distinctive morphological changes, SO_2 interacted more with oily substances and styrene-acrylic films showed a higher sensitivity to degradation reactions in combination with humidity. Middleton et al. [30] studied how polymer degradation was influenced by ozone at elevated and at room temperatures and how it compared to aging in air at high temperatures. It was

found that at a temperature of 140 °C and for an aging duration of 90 days the effect of 1% ozone can be disregarded, since the high temperature is the driving force of the degradation process. However, it is believed that for shorter periods of time and lower temperatures closer to bitumen field conditions the impact of ozone and other ROS on the aging process is more severe. Focusing on the determination of the underlying mechanisms of oxidation Hoffmann et al. [31] investigated photo-oxidation of hydrocarbons, whereby laser pulses initiated the oxidation process and a time resolved detection of OH and NO_2 radicals was performed. With this technique the oxidation rates and products of hydrocarbons can be observed and it can be applied to the study of volatile organic compounds (VOC), which occur in bituminous materials. Furthermore, field studies with polymers and with bitumen have been performed, thereby naturally incorporating sunlight, moisture and atmospheric ROS. The aging of polyethylene and styrene-butadiene was investigated by Getlichermann et al., who exposed polymer films directly to solar radiation for 15 days to uncover specific degradation mechanisms in polymers [32]. Soenen et al. [33] examined the rheological and chemical properties of field aged binders, showing similar trends between field and laboratory aged samples when looking at the stiffness and the carbonyl index. However, the aging level of the field aged samples surpassed the laboratory aged samples, indicating that more advanced aging methods could lead to a better correlation. Masson et al. [34] performed a field study with styrene-butadiene modified bitumen used as sealants, whereby samples were collected after one, three, five and nine years of service and then subjected to physico-chemical analysis. Occurring aging processes were confirmed to result in the formation of sulphoxides, sulphones, ketones and carboxylic acids, in the loss of aromatics and in block copolymer degradation. It is reported that the performance of the investigated bituminous sealants did not correlate well with standard aging tests, since these could not predict the performance of the materials under natural weathering conditions. The authors therefore recommended developing a more realistic aging method for bituminous materials.

The process of developing an aging method for bitumen that is time-efficient and as close to reality as possible has been gaining more attention in the last years. Hofko et al. [35] investigated the impact of ROS on asphalt mixtures by exposing the asphalt mix specimen to air, O_2, O_3 and NO_x. The results show that O_3 alone does not have a high oxidation potential, but in combination with NO_x heavy aging is being induced. Furthermore, the effect of ROS on bitumen was studied by Mirwald et al. [36, 37], who developed the Viennese Binder Aging (VBA) method [38] by adapting the previously developed Viennese Aging Procedure (VAPro) for asphalt mixtures [39, 40]. During this aging method the bitumen samples are kept at 80 °C, which correlates with field conditions, and exposed to air enriched with O_3 and NO_x. Although the main aging inducing factors during VBA are the high concentrations of O_3 and NO_x at elevated temperatures, the goal is to further advance the aging setup and incorporate as many aging inducing factors as possible occurring in the environment. It has been shown that ROS play an important role in the aging process of bitumen, but the specific impact of each gas species (and possible cooperative effects) have not yet been identified.

The purpose of this study was the determination and comparison of the effect of single ROS on bitumen aging. Therefore, three unmodified short-term aged bitumen were long-term aged using an adapted version of the VBA method [38], which allows the separate exposure of the sample to O_3, NO and NO_2 in different carrier gases. These experiments were then compared to standardized aging methods (RTFOT + PAV). The properties of the binders after aging were characterized using Fourier-Transform-Infrared (FTIR) spectroscopy and the dynamic shear rheometer (DSR). FTIR is a very helpful tool for the assessment of the chemical composition of bituminous materials and has been used progressively in the last two decades. Together with the mechanical information obtained from the DSR measurements the chemo-mechanical correlation of the acquired data can be determined.

2 Materials and Methods

2.1 Materials

For this study, three non-modified binders with the penetration grade 70/100 were used, whereby each binder was provided by a different refinery. Their basic properties are summarized in Table 1.

Table 1 Properties of binders used for study

Binder	Refinery	Penetration grade (1/10 mm)	Performance grade (°C)	Softening point (°C)
A	A	84	58–28	45.8
B	B	77	58–28	45.6
C	C	73	64–28	46.6

Several aging methods were performed and the binders were then analysed in their respective aging states: a) unaged, b) short-term aged and c) long-term aged. The standardized methods used were the Rolling Thin Film Oven Test (RTFOT) according to EN 12607–1 [8] for STA and the Pressure Aging Vessel (PAV) at 100 °C according to EN 14769 [9] for LTA. Furthermore, PreVBA was used for STA and an adapted version of the VBA method for LTA. A detailed explanation of these methods will follow below.

2.2 Methods

2.2.1 "Pre " Viennese binder aging (PreVBA)

For the "Pre" Viennese binder aging (PreVBA) method the respective bitumen was heated up to ~ 110 °C in a small metal can for approximately 5 min and stirred with a thermometer for homogenization and temperature detection. After reaching the desired temperature, 8 g of the material were poured into a PAV metal container as evenly as possible and then transferred into a ventilated oven, where the sample was kept at 163 °C for 75 min (similar to the conditions during RTFOT). The purpose of PreVBA is not only to achieve a STA condition, but also to prepare the sample, as it results in a uniformly distributed bitumen film with a thickness of 0.5 mm. (Fig. 1). After PreVBA the bitumen sample is transferred into the VBA aging cell for LTA.

2.2.2 Viennese binder aging (VBA)

The VBA is an aging method introduced by Mirwald et al. [38] as a way to simulate LTA of bitumen in a more realistic way using ROS in combination with an elevated temperature as aging inducing factors. More detailed information on the reason for incorporating ROS, on the separate parts of the aging setup and the reactions taking place between bitumen and the different gas species can be obtained directly from Mirwald et al. [38]. In this method an ozone generator operated with air is used to produce O_3 and NO_x, which are then led into an aging cell made out of stainless steel. Since the focus of the current study was to investigate the effect of single ROS on bitumen aging the VBA setup was adapted to allow separate exposure of the sample to O_3, NO and NO_2 (see Fig. 2). Therefore, gas bottles with different concentrations of NO in N_2 and NO_2 in air and N_2 were connected to the aging cell. For the production of O_3 without the presence of NO_x and to keep the overall oxygen content in the atmosphere approximately at the same level as in air, the ozone generator was operated with a mixture of 79% argon and 21% oxygen. The ozone generator was the type COM-AD-01 and the ozone analyzer, which was used for the determination of the ozone concentration in the gas flow, was the GM-OEM both from the company ANSEROS.

Each binder was exposed to 21 different atmospheres, whereby two bitumen films were aged simultaneously in order to increase efficiency. The composition of the respective atmospheres was as follows:

- 50, 100, 200, 400 and 600 ppm of NO in N_2
- 50, 100, 200, 400 and 600 ppm of NO_2 in air and in N_2
- 2, 5, 8 and 10 g/m^3 O_3 in a mixture of 21% O_2 and 79% Ar
- 21% O_2 and 79% Ar
- N_2

NO_2 in N_2 provides information about the aging behavior of NO_2 as the sole oxygen source and NO_2 in air about the aging behavior of NO_2 together with O_2. To allow a better comparison between the different ROS, 2, 5, 8 and 10 g/m^3 O_3 can be approximately converted into 1207, 3019, 4830 and 6037 ppm of O_3 in the corresponding atmosphere. For reference, the national alarm level of ozone in the atmosphere is about four orders of magnitude lower at 240 µg/m^3

Fig. 1 Bitumen in metal container before (left) and after (right) PreVBA

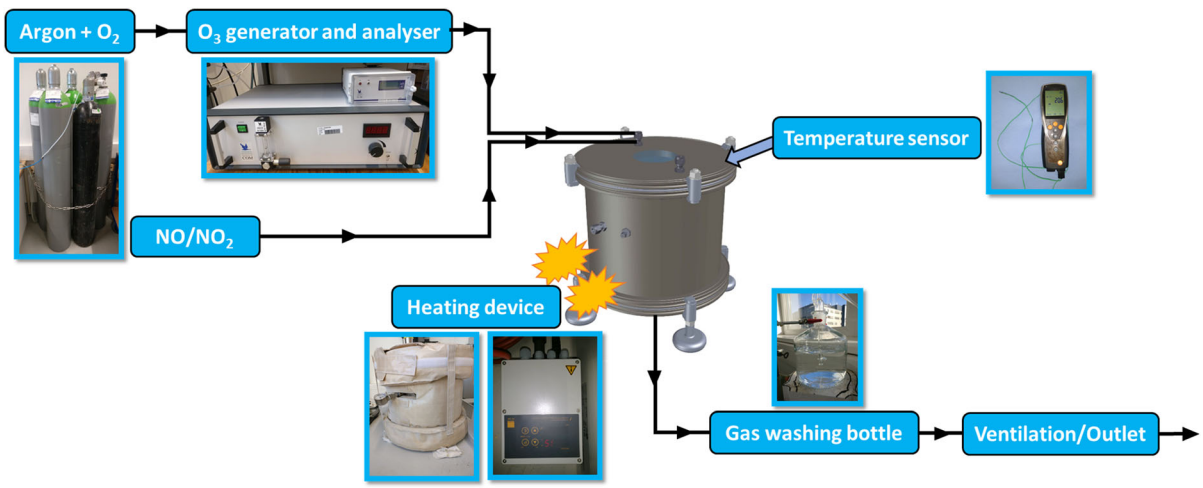

Fig. 2 Adapted setup allowing separate introduction of O_3, NO_2 and NO into the aging cell

[41] and the average annual value for NO_2 is set at 30 µg/m^3 [42]. All experiments were conducted at 80 °C, with an aging duration of 3 days and a gas flow of 50 ± 5 l/h, whereby the flow rate was modulated with floating ball flow meters.

2.2.3 *Attenuated total reflection fourier-transformation infrared (ATR-FTIR) spectroscopy*

For the detection of changes in the chemical composition FTIR spectroscopy was used. The respective bitumen samples were heated up to ∼ 110 °C in a spoon and stirred with a thermometer for homogenization and temperature detection. After reaching the desired temperature small droplets of sample were transferred on a silicone foil. The sample preparation is shown in Fig. 3.

For the measurement a Bruker Alpha II with an DTGS detector and an attenuated total reflection (ATR) unit containing a diamond crystal was used. The ATR geometry allows the recording of FTIR spectra in adsorption equivalent mode and the bitumen samples can be applied directly onto the crystal in solid state. All spectra were measured from 4000–400 cm^{-1} at a resolution of 4 cm^{-1} (24 scans)

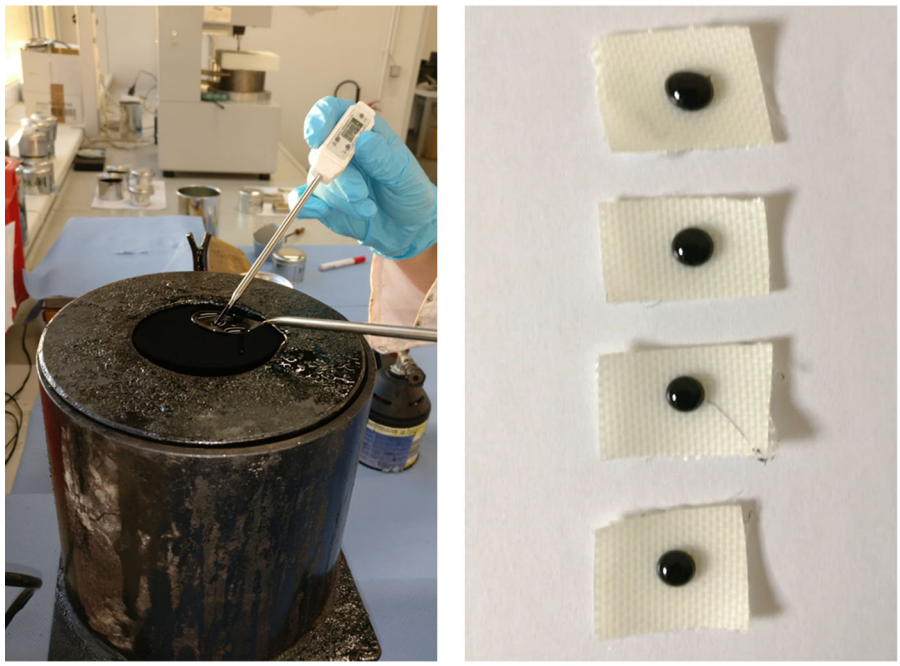

Fig. 3 ATR-FTIR sample preparation

with four repetitions. For each aging state (which corresponds to a different atmosphere during VBA) four samples were prepared, resulting in 16 spectra per aging state. Each ATR-FTIR-measurement consisted out of the following steps: Firstly, the ATR crystal was cleaned with limonene and isopropanol and then a background spectrum was recorded. After applying the bitumen sample on the ATR crystal, the spectra were recorded. For spectra evaluation and processing the software OPUS was used. A normalization between 3200–2800 cm^{-1} was carried out and a full base line integration using the following frequency limits was performed:

- Carbonyls (AI_{CO}): 1660–1800 cm^{-1}
- Sulfoxides (AI_{SO}): 1079–984 cm^{-1}
- Reference aliphatic band (AI_{CH3}): 1525–1350 cm^{-1}

By calculating the Aging Index (AI) according to Eq. 1 the uptake in oxygen due to the aging process can be assessed.

$$AI_{FTIR} = \frac{(AI_{CO} + AI_{SO})}{AI_{CH_3}} \quad (1)$$

The AI of each aging state shown in this paper is obtained by determining the mean value and standard deviation of the respective 16 spectra.

2.2.4 *Dynamic shear rheometer (DSR)*

For the detection of changes in the mechanical properties the DSR was used. The samples were heated up to ~ 110 °C in a small metal can and stirred with a thermometer for homogenization and temperature detection. After reaching the desired temperature the bitumen sample was poured into a silicone mold and stored in the dark for 24 h. The measurements were conducted with an MCR 302 Anton Paar DSR according to EN 14770 [43] as a frequency sweep at the following frequencies and temperatures:

- 0.1, 0.3, 1, 1.592, 3, 5, 8 and 10 Hz
- 40, 46, 52, 58, 64, 76 and 82 °C

2.2.5 *2.2.5 Chemo-mechanical correlation*

The chemo-mechanical correlation illustrates the link between the mechanical properties and the chemical composition of the respective bitumen sample. The

FTIR aging index, which represents the formation of carbonyls and sulfoxides, is plotted on the X-axis and the norm of the complex modulus |G*| or the phase angle δ is plotted on the Y-axis. This gives visual and graphical information about how an increase in stiffness is correlated to an increase in incorporated oxygen and vice versa. For this study |G*| at 1.592 Hz and 46 °C is used for the chemo-mechanical correlation.

3 Results and discussion

3.1 NO in N_2

The impact of NO on bitumen aging was investigated by exposing the samples to an aging atmosphere consisting of N_2 with different concentrations of NO for 3 days at 80 °C. In Fig. 4 the chemo-mechanical correlation of the three binders is displayed. The results show that the values for |G*| and AI_{FTIR} are very close to the STA state, which indicates that no significant aging took place, regardless of the level of NO in the aging cell. For all three binders the DSR and FTIR measurements displayed no distinctive aging trend after aging with NO, indicating no dependency on the bitumen source or composition. The scattering between the data points for the different NO concentrations is in the expected range and can be explained by naturally occurring variations between experiments, e.g. inhomogeneity of the bitumen sample and fluctuations in gas flow or temperature. In principal, NO plays an important role in atmospheric photochemical processes including decomposition of ozone and the tropospheric cycle of OH radicals [44, 45], however, NO is not an oxidizing agent and other reactants and also energy input through radiation are required for these reaction cycles. Therefore, it is assumed that higher nitrogen oxides or other strong oxidants have to be present for a reaction with bitumen to take place.

3.2 NO_2 in N_2

The chemo-mechanical correlation for the three binders after 3 days in N_2 + NO_2 is shown in Fig. 5. By using NO_2 instead of NO oxidation occurs, causing the |G*| and AI_{FTIR} to rise. When looking at the results, it can be seen that the complex modulus is increasing proportionally with the NO_2 concentration for all three binders. Binder A and B show very similar trends with an average gap of 7 kPa between the different concentrations and binder C shows a slightly stronger increase of |G*| with an average gap of 14 kPa. The highest value for the complex modulus is obtained after 3 days in N_2 + 600 ppm NO_2, surpassing the PAV aged sample by approximately 5 kPa for binder A, 7 kPa for binder B and 20 kPa for binder C. Based on the more distinct increase in |G*| and the considerably higher aging level after 600 ppm NO_2 compared to after PAV aging it can be assumed that binder C might be more susceptible to oxidation induced by NO_2 in N_2.

However, when looking at the aging index the values partly deviate from the expected trend that a higher concentration of NO_2 leads to a higher aging level. In Fig. 6 it can be seen that for binder A the AI_{FTIR} is increasing from 0.363 for 50 ppm, to 0.378 for 100 ppm and to 0.380 for 200 ppm NO_2. However, for 400 and 600 ppm the AI_{FTIR} is decreasing to 0.376

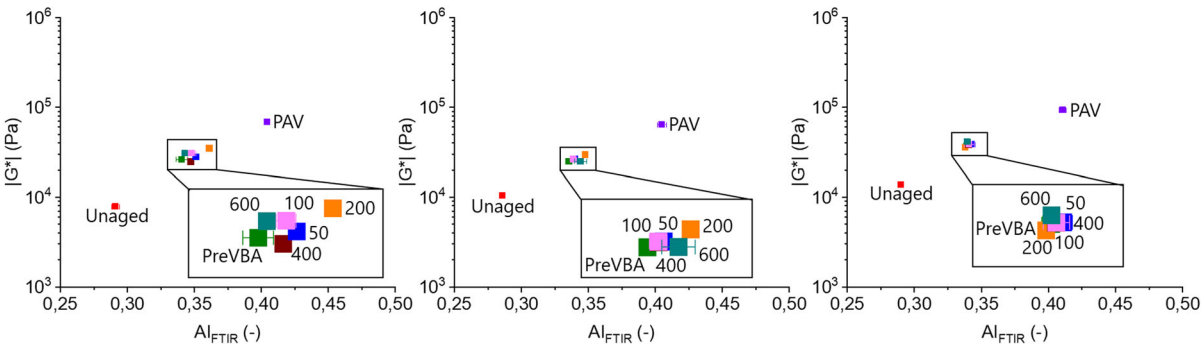

Fig. 4 Chemo-mechanical correlation of binder A (left), binder B (middle) and binder C (right) after 3 days in N_2 + NO at 80 °C; concentrations in ppm

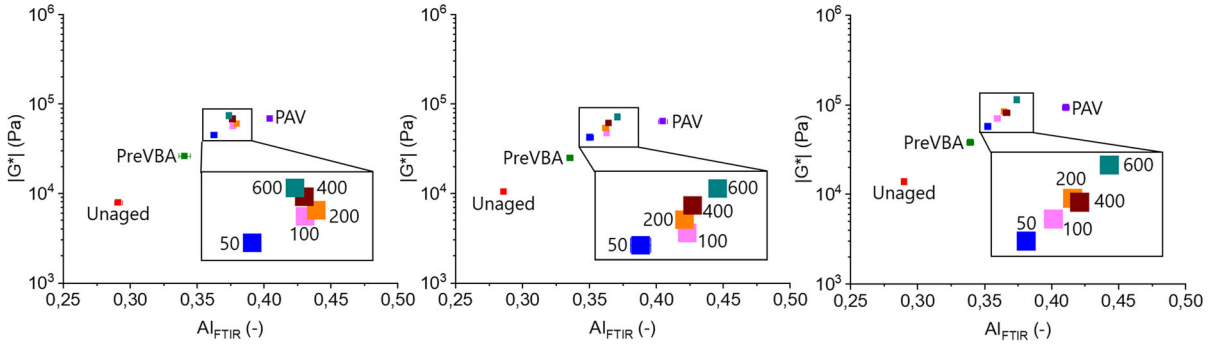

Fig. 5 Chemo-mechanical correlation of binder A (left), binder B (middle) and binder C (right) after 3 days in N_2 + NO_2 at 80 °C; concentrations in ppm

and then to 0.374. The behavior of binder A can be explained by looking at the FTIR spectra.

The aging index, which is used for the chemo-mechanical correlation, is calculated according to Eq. 1. When looking at the FTIR spectra of binder A (see Fig. 6), it can be seen that the sulfoxide band does not increase proportionally with the NO_2 concentration, but decreases, which results in lower aging indices. However, in the range of 1350–1100 cm^{-1} the absorption of the bitumen samples follows the expected trend by showing the highest absorption for 600 ppm NO_2 and the lowest for 50 ppm NO_2. The decreasing sulfoxide band could be explained by subsequent reactions to sulfones or decomposition of the sulfoxides. Therefore, it is possible that the bitumen sample after 3 days in N_2 + 600 ppm NO_2 did incorporate the highest amount of oxygen during the aging process, but this is not properly detected by the current definition of the FTIR aging index, as it merely includes carbonyls and sulfoxides. Unfortunately, this problem has not yet been solved, since it is not clear what bands result from the formation of specific chemical compounds and what bands increase simply because of a general rise in polarity in the material.

The FTIR spectra and aging index of binder B are depicted in Fig. 7. Contrary to binder A, the sulfoxide band of binder B between 1079 and 984 cm^{-1} increases with the NO_2 concentration, showing the lowest intensity for 50 ppm NO_2 (in blue) and the highest for 600 ppm NO_2 (in turquoise). Additionally, the area from 1350 to 1100 cm^{-1} follows the same trend, whereby the bands of the different concentrations can be seen even more clearly here. The spectrum after 50 ppm NO_2 at the bottom in blue, then 100 ppm NO_2 in pink, 200 ppm NO_2 in orange,

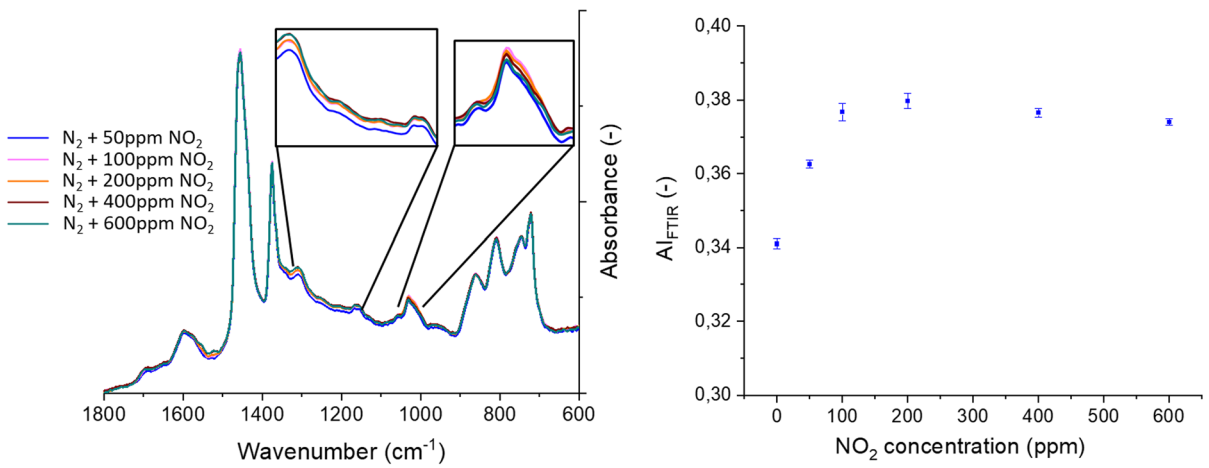

Fig. 6 FTIR spectra and aging index of binder A after aging with different concentrations of NO_2 in N_2

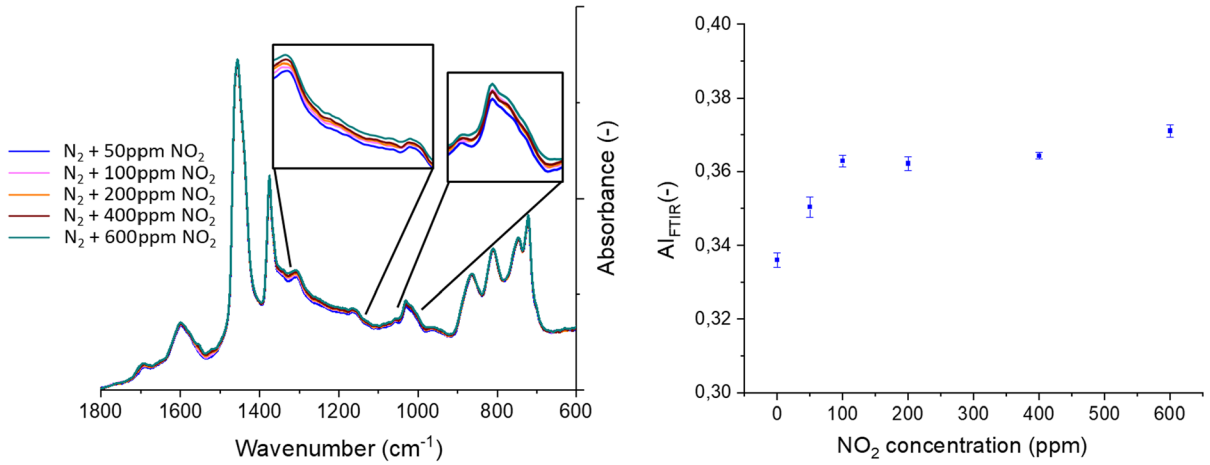

Fig. 7 FTIR spectra and aging index of binder B after aging with different concentrations of NO_2 in N_2

400 ppm NO_2 in brown and 600 ppm NO_2 in turquoise on the top. The increasing sulfoxide band in combination with the increasing carbonyl band results in a steadily rising aging index from 0.336 for 0 ppm to 0.371 for 600 ppm NO_2, as opposed to the decreasing aging index of binder A. This could be explained by the fact, that the sulfoxides formed in binder B are not as prone to decomposition or additional reactions as the sulfoxides in binder A and can therefore be detected with ATR-FTIR at the end of the aging experiment. The reason for that could be the different crude oil source of binder A and B, which results in a different chemical composition and therefore in a chemical environment for the sulfoxides, where they might be more stable or the possibility for further reactions is not given. Another interesting observation in Fig. 7 is the very steep increase of AI_{FTIR} from 0 to 100 ppm NO_2, which then transitions into a less distinct incline for 100 to 600 ppm. Two hypotheses have been established for the explanation of this phenomenon: Firstly, it is possible that the aging process is accelerated immensely by the addition of NO_2, though minor concentrations of NO_2 are sufficient and higher amounts only have a slight effect. Secondly, a similar problem as observed for binder A might occur, whereby higher concentrations of NO_2 could indeed cause more aging, however this is concealed by the current definition of AI_{FTIR}.

In Fig. 8 the FTIR spectra and aging index of binder C can be seen. The bands follow the same trend that was observed for binder B (see Fig. 7). The sulfoxide band between 1079 and 984 cm^{-1} and the area between 1350 and 1100 cm^{-1} show the highest intensity for the highest NO_2 concentration, which leads to an increase in the aging index from 0.352 to 0.374 from 50 to 600 ppm of NO_2. This indicates that binder B and C might have a more similar chemical composition compared to binder A, which causes the sulfoxides to be more stable and/or less reactive. On the right hand-side of Fig. 8 the AI_{FTIR} is depicted as a function of the NO_2 concentration. The same steep rise of the aging index followed by a weaker increase, as was seen for binder B, can be observed here, although the flattening of the slope is slightly less distinctive for binder C. This could be explained by the fact, that binder C has to some extent a higher aging susceptibly under these aging conditions, resulting in a more pronounced effect at higher concentrations of NO_2.

3.3 NO_2 in air

The chemo-mechanical correlation for the binders after 3 days in air + NO_2 is shown in Fig. 9. The addition of NO_2 to air leads to heavy oxidation, causing a very high complex modulus and aging index in all the samples. When looking at the results for binder A on the left hand-side an almost linear increase in |G*| with AI_{FTIR} can be observed. The addition of 50 ppm NO_2 to the aging atmosphere results in an aging index of 0.439 and a |G*| of 119 kPa, whereby the PAV aged level is surpassed by 0.035 and 51 kPa, respectively. From 50 to 100, from 100 to 200 and from 200 to 400 ppm of NO_2 the AI_{FTIR} increases on average by 0.005 and the |G*| by 30 kPa. The most

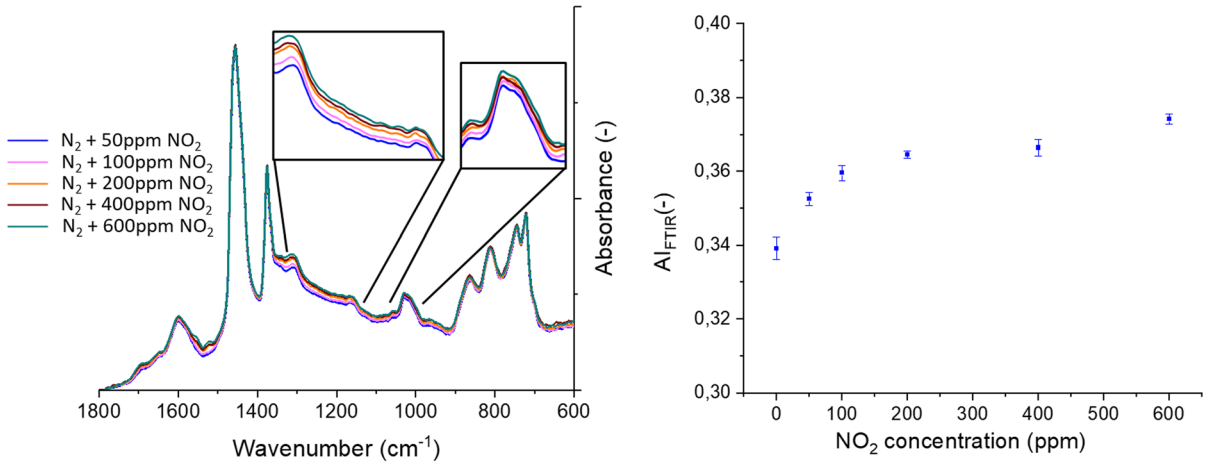

Fig. 8 FTIR spectra and aging index of binder C after aging with different concentrations of NO_2 in N_2

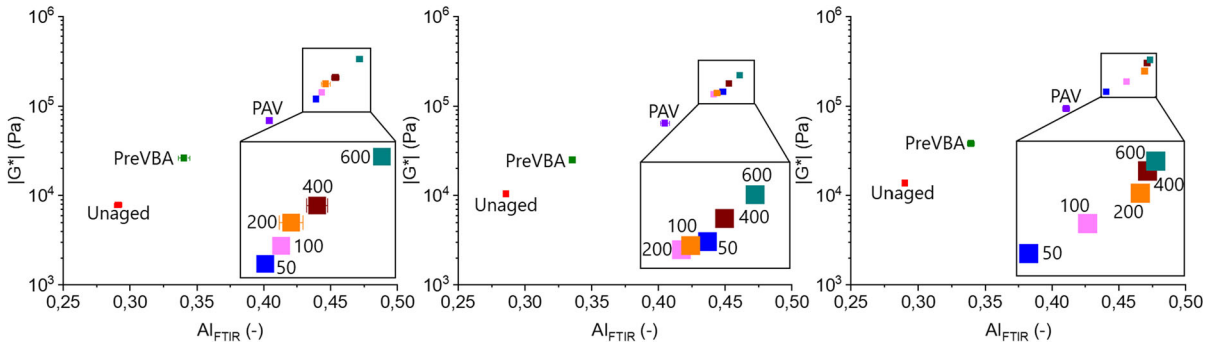

Fig. 9 Chemo-mechanical correlation of binder A (left), binder B (middle) and binder C (right) after 3 days in air + NO_2 at 80 °C; concentrations in ppm

significant increase is observed for the step from 400 to 600 ppm of NO_2, whereby the AI_{FTIR} goes up by 0.018 and the |G*| by 124 kPa. From the STA state (after PreVBA) to the LTA state achieved after 3 days in air + 600 ppm NO_2 the ΔAI_{FTIR} is 0.131 and Δ|G*| is 306 kPa.

For binder B the chemo-mechanical correlation also shows a linear trend, with the largest gap between 400 and 600 ppm. However, the increase in aging index and complex modulus is with 0.008 and 42 kPa significantly lower than for binder A. Moreover, the data points for 50, 100 and 200 ppm of NO_2 are especially close together, with the results for 50 ppm even surpassing 100 and 200 ppm of NO_2. This could be explained by binder B having a lower aging susceptibility for NO_2 concentrations up to 200 ppm, where in that range the exact concentration has no influence on the aging level. However, the more likely explanation is that the sample underwent additional aging during storage, processing or analysis in the course of the aging experiment with 50 ppm NO_2 and that this sample shows therefore an unexpectedly high AI_{FTIR} and |G*|. From the STA state (after PreVBA) to the LTA state achieved after 3 days in air + 600 ppm NO_2 the ΔAI_{FTIR} is 0.125 and Δ|G*| is 195 kPa. When comparing these results to binder A the increase of the aging index is very similar, however for the |G*| binder A shows a significantly higher increase.

When looking at the chemo-mechanical correlation for binder C, it shows a linear correlation between the aging index and the complex modulus, however the largest gap with ΔAI_{FTIR} = 0.015 and Δ|G*|= 58 kPa occurs from 50 to 100 ppm. The impact of the increase in NO_2 concentration is becoming less significant for the higher concentrations, especially for 200, 400 and 600 ppm with an average ΔAI_{FTIR} of 0.005 and an

average Δ|G*| of 35 kPa. Most notably is the very minor increase in the aging index, indicating a smaller amount of incorporated oxygen or that the incorporated oxygen could not be as well detected for binder C as for binder A and B. From the STA state (after PreVBA) to the LTA state achieved after 3 days in air + 600 ppm NO_2 the ΔAI_{FTIR} is 0.134 and Δ|G*| is 288 kPa, whereby the increase in the aging index is very similar to the other two binders and the increase in the complex modulus is very similar to the increase observed for binder A. Although the three investigated binders show some differences, it can be said that overall the influence of NO_2 in air on the aging process is the same. The added NO_2 causes a drastic increase in the occurring oxidation, therefore inducing the formation of ketones and sulfoxides. Furthermore, the complex modulus is increasing significantly making the sample stiffer and more brittle after the aging process. As of now, it is assumed that NO_2 acts as a "door opener" for the oxidation process in this setting, enabling increased oxidation reactions with the O_2 from the air [46]. It is possible that NO_2 decreases the activation energy for a reaction of O_2 with bitumen or that elevated oxygen states are formed through reactions of NO_2 with O_2. These elevated oxygen states hold a higher energy and an oxidation reaction with bitumen is therefore facilitated.

3.4 O_3 in Ar + O_2

The chemo-mechanical correlation for the binders after 3 days in 21% O_2 + 79% Ar + O_3 is displayed in Fig. 10. As already mentioned the reason for using a mixture of O_2 and Ar was firstly to allow the production of O_3 without the presence of NO_x and secondly to keep the overall oxygen content in the atmosphere approximately at the same level as in air. When looking at the chemo-mechanical correlation of binder A on the left hand-side, it can be seen that with an average AI_{FTIR} of 0.413 and an average |G*| of 69 kPa all experiments led to aging levels close to the PAV with AI_{FTIR} = 0.404 and |G*|= 68 kPa. The data point for 2 g/m^3 of O_3 is shifted somewhat to a higher aging index and complex modulus, however minor deviations can be explained by additional aging that occurred during storage, processing or analysis. For binder A the exposure to higher O_3 concentrations did not result in a significant increase or decrease AI_{FTIR} or |G*|, indicating that the O_3 concentration does not have a strong influence on the aging process.

Very similar results can be seen when looking at the chemo-mechanical correlation for binder B in the middle of Fig. 10. With an average AI_{FTIR} of 0.409 and an average |G*| of 70 kPa the aging experiments with O_3 led approximately to the PAV aging level of AI_{FTIR} = 0.405 and |G*|= 64 kPa. The scattering between the data points of different O_3 concentrations is also in the expected range, suggesting that the addition of more O_3 does not cause more aging to occur.

However, the chemo-mechanical correlation of binder C shows a different trend. The experiment with 2 g/m^3 of O_3 induced approximately the same amount of oxidation and stiffening as the PAV method, but contrary to binder A and B higher concentrations of O_3 did cause a rise in the aging index and complex modulus by an average of 0.012 and 15 kPa. This indicates that binder C is more

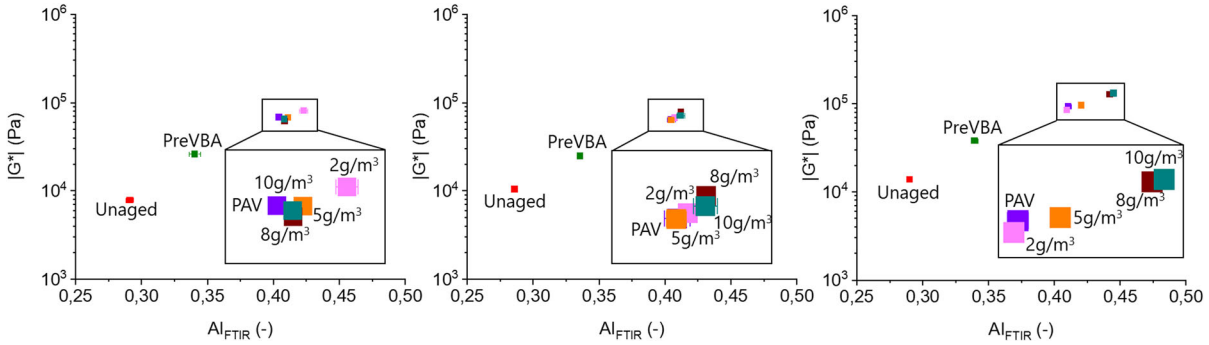

Fig. 10 Chemo-mechanical correlation of binder A (left), binder B (middle) and binder C (right) after 3 days in Ar + O_2 + O_3 at 80 °C

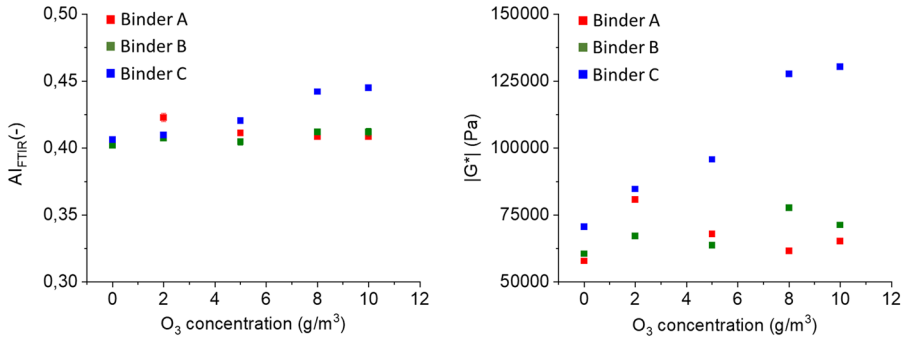

Fig. 11 AI_{FTIR} (left) and |G*| (right) of binder A, B and C with different concentrations of O_3 in Ar + O_2

susceptible for oxidation reactions with O_3, which could be caused by differences in the chemical composition due to the specific crude oil source or production process.

A more detailed depiction of the influence of O_3 on the aging process can be obtained from Fig. 11, where the correlation between the AI_{FTIR} and the O_3 concentration (left) and between |G*| and the O_3 concentration (right) is depicted.

For binder A and B, the addition of O_3 to the atmosphere in the aging cell does not cause a higher aging index or complex modulus. A possible explanation is that due to the high oxidation potential of O_3 the surface of the bitumen sample immediately oxidizes and thus, a passivation layer is formed. Subsequently, O_3 does not induce any oxidation of the bulk, leading to a constant AI_{FTIR} and |G*|. A different picture is given when looking at the results for binder C, which show a consistent rise of AI_{FTIR} and |G*|. A reason for this difference in the aging behaviour could be the previously mentioned variations in the chemical composition between the binders. An organic compound with a high susceptibility for an oxidation reaction with O_3 could be responsible for the formation of said passivation layer. A possibility for that would be chemical structures containing unsaturated hydrocarbons, whereby an ozonolysis of the double bond takes place. Thereby, a ozonide is formed as an intermediate, which then further reacts to an aldehyde, a ketone or also to a carboxylic acid (see Fig. 12) [47].

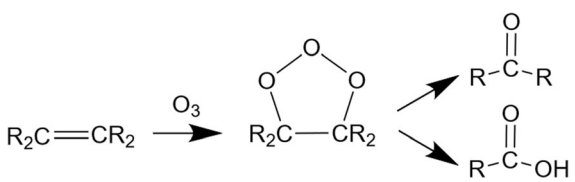

Fig. 12 Oxidation reaction with O_3 adapted from [47]

If binder A and B show a significant higher concentration of e.g. unsaturated hydrocarbons, it is possible that the formed passivation layer on the surface of binder A and B is significantly thicker than on the surface of binder C. That could subsequently explain why binder C shows an increase in AI_{FTIR} and |G*| with the O_3 concentration while binder A and B do not show this dependency. However, to determine this kind of information the application of other more suitable chemical analysis methods, e.g. nuclear magnetic resonance spectroscopy (NMR) or also mass spectrometry, would be necessary.

3.5 Comparison of different atmospheres

In the previous chapters the impact of selected ROS on bitumen aging was discussed in detail. The comparison of these different ROS and the associated aging atmospheres is displayed in Fig. 13, where very similar trends for all three binders can be observed. The aging index and the complex modulus after 3 days in N_2 + 600 ppm NO are in close proximity to the values after STA with PreVBA. This indicates that NO as the only oxygen source induces no aging, neither by a formation of carbonyls or sulfoxides, nor in the form of an increase in stiffness. When looking at the results for 3 days in N_2 + 600 ppm NO_2 and 3 days in 21% O_2 + 79% Ar + 10 g/m^3 of O_3 it can be seen that although both experiments lead to approximately the same |G*| for all three binders, the AI_{FTIR} shows different values. For binder A the ΔAI_{FTIR} for the aging experiment with NO_2 and with O_3 is 0.034, for binder B it is 0.041 and for binder C it is 0.071. This means that in these cases an increase of the AI_{FTIR} and

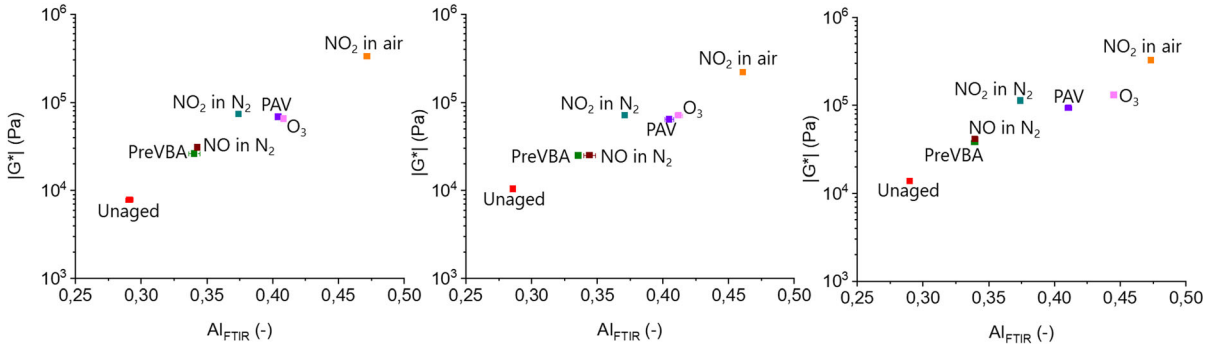

Fig. 13 Comparison of different aging atmospheres for binder A (left), binder B (middle) and binder C (right); the concentration of the respective ROS species is 600 ppm (NO, NO_2) and 10 g/m^3 (O_3)

therefore an increase of carbonyls and sulfoxides in the bitumen sample does not go hand in hand with an increase in stiffness. A possible explanation is that not only carbonyls and sulfoxides are formed but also other changes in the chemical composition occur, which compensate the increasing polarity gradient and therefore the material does not become stiffer. The increase of AI_{FTIR} compared to the aging experiments with NO_2 in N_2 is believed to be caused by the additional O_2 in the aging cell. While all three binders showed significant aging in N_2 + 600 ppm of NO_2, the biggest impact was caused by the addition of 600 ppm of NO_2 to air, with an average ΔAI_{FTIR} of 0.096 and an average $\Delta|G^*|$ of 207 kPa in comparison to the same concentration of NO_2 in N_2. The results show that NO_2 does induce a certain amount of aging when being the sole oxygen source, but its full oxidation potential is unfolded with an additional oxygen source present.

4 Conclusion

Understanding the aging processes in bitumen is a crucial aspect in making bituminous construction materials more durable, enabling successful recycling and prolong its overall service life time. Therefore, aging methods that are as close to reality as possible, need to be considered. Aging inducing factors that are not being taken into consideration in standard LTA methods, are humidity, light and ROS, whereby especially ROS have been greatly disregarded. Therefore, the effect of NO, NO_2 and O_3 on three unmodified bituminous binders has been investigated in this study. This was achieved by adapting the VBA method to allow separate exposure to NO, NO_2 and O_3 in different atmospheres and analysing the respective bitumen samples with ATR-FTIR spectroscopy and with the DSR.

The results show that while NO in N_2 does not induce any significant aging, NO_2 in N_2 causes oxidation reactions to occur, resulting in an increase in AI_{FTIR} and $|G^*|$. This means that the oxidation potential of NO_2 is sufficiently high to cause aging in bituminous binders, even with NO_2 as the sole oxygen source in the system. The addition of O_3 to the atmosphere did not have any effect on the aging process of binder A and B, but for binder C a dependency of AI_{FTIR} and $|G^*|$ on the O_3 concentration was seen. A possible explanation for this observation could be differences in the chemical composition and therefore in the aging susceptibility regarding different ROS of the three binders. Furthermore, the comparison of the different aging atmospheres showed that NO_2 in N_2 and O_3 in Ar + O_2 induced an approximately equal rise in the $|G^*|$ for all three binders. However, the experiments with O_3 resulted in a higher AI_{FTIR}, which is assumed to be caused by the additional O_2 in the aging cell.

The most significant impact was observed for the addition of NO_2 to air, whereby the AI_{FTIR} and $|G^*|$ of all other aging experiments were greatly surpassed. The results indicate that in combination with an additional oxygen source NO_2 acts as an oxidation intensifier or accelerator. For a more detailed analysis of the underlying mechanisms and to find more comprehensive explanations for the specific aging behaviour of the binders, additional chemical analysis methods, e.g. NMR or fluorescence spectrometry, will be used in the future. Especially, the connection of a

SARA separation of the aged bitumen samples and a subsequent examination of the different fractions with the previously stated analytical methods could provide a deeper insight.

Moreover, the combination of ROS in different ratios could lead to more severe aging and could offer more information about how bituminous products age during their service life. The VBA aging method could be further modified to include moisture and light, thereby providing a realistic aging setup for not only bituminous materials, but also for any other materials exposed to atmospheric aging and weathering. Certain questions about the aging of bitumen are still unanswered, but this study provides evidence that ROS play an important role and should not be disregarded when looking at the aging of bituminous materials.

Funding Open access funding provided by TU Wien (TUW). The financial support by the Austrian Federal Ministry for Digital and Economic Affairs, the National Foundation for Research, Technology and Development and the Christian Doppler Research Association is gratefully acknowledged. Furthermore, the authors would also like to express their gratitude to the CD laboratories company partners BMI Group, OMV Downstream and Pittel + Brausewetter for their financial support.

Declarations

Conflict of interest No potential conflict of interest was reported by the authors.

References

1. Read J, Whiteoak D (2003) The shell bitumen handbook. Thomas Telford
2. Speight JG (2006) The chemistry and technology of petroleum. CRC Press
3. McIntosh J (2008) The ancient Indus Valley: new perspectives. Abc-Clio
4. Abraham H (1918) Asphalts and allied substances: their occurrence, modes of production, uses in the arts and methods of testing. D. van Nostrand
5. Bitumen S (1995) The shell bitumen industrial handbook. Thomas Telford
6. Lesueur D (2009) The colloidal structure of bitumen: Consequences on the rheology and on the mechanisms of bitumen modification. Adv Coll Interface Sci 145(1):42–82
7. JP P, A review of the fundamentals of asphalt oxidation
8. CEN (2015) EN 12607–1 Bitumen and bituminous binders-Determination of the resistance to hardening under the influence of heat and air-Part 1: RTFOT method, Brussels
9. CEN (2012) EN 14769: Bitumen and bituminous binders-Accelerated long-term ageing conditioning by a pressure ageing vessel (PAV). Brussels
10. Valentin J et al (2021) A comprehensive study on adhesion between modified bituminous binders and mineral aggregates. Constr Build Mater 305:124686
11. Cong P, Guo X, Ge W (2021) Effects of moisture on the bonding performance of asphalt-aggregate system. Constr Build Mater 295:123667
12. Valentová T, Altman J, Valentin J (2016) Impact of asphalt ageing on the activity of adhesion promoters and the moisture susceptibility. Transp Res Procedia 14:768–777
13. Airey GD et al (2008) The influence of aggregate, filler and bitumen on asphalt mixture moisture damage. Constr Build Mater 22(9):2015–2024
14. Zou Y et al (2021) Effect of different aqueous solutions on physicochemical properties of asphalt binder. Constr Build Mater 286:122810
15. Ma L et al (2021) Comprehensive review on the transport and reaction of oxygen and moisture towards coupled oxidative ageing and moisture damage of bitumen. Constr Build Mater 283:122632
16. Das PK et al (2015) Coupling of oxidative ageing and moisture damage in asphalt mixtures. Road Mater Pavement Design 16(sup1):265–279
17. López-Montero T, Miró R (2016) Differences in cracking resistance of asphalt mixtures due to ageing and moisture damage. Constr Build Mater 112:299–306
18. Huang SC, Turner T, Thomas K (2008) The influence of moisture on the aging characteristics of bitumen. In: Proceedings of the 4th eurasphalt and eurobitume congress held may 2008, Copenhagen, Denmark
19. Li Y et al (2019) Aging effects of ultraviolet lights with same dominant wavelength and different wavelength ranges on a hydrocarbon-based polymer (asphalt). Polym Test 75:64–75
20. Hu J et al (2018) Effect of ultraviolet radiation in different wavebands on bitumen. Constr Build Mater 159:479–485
21. Mirwald J, et al. (2022) Time and storage dependent effects of bitumen—comparison of surface and bulk. In: proceedings of the RILEM international symposium on bituminous materials. 2022. Cham: Springer International Publishing
22. Mirwald J et al (2022) Impact of UV–Vis light on the oxidation of bitumen in correlation to solar spectral irradiance data. Constr Build Mater 316:125816
23. Feng Z-G et al (2016) FTIR analysis of UV aging on bitumen and its fractions. Mater Struct 49(4):1381–1389

24. Feng Z-G et al (2013) Effect of ultraviolet aging on rheology, chemistry and morphology of ultraviolet absorber modified bitumen. Mater Struct 46(7):1123–1132
25. Feng Z et al (2020) Aging properties of ultraviolet absorber/SBS modified bitumen based on FTIR analysis. Construct Build Mater. https://doi.org/10.1016/j.conbuildmat.2020.121713
26. Naskar M et al (2013) Effect of ageing on different modified bituminous binders: comparison between RTFOT and radiation ageing. Mater Struct 46(7):1227–1241
27. Jacob DJ (2000) Heterogeneous chemistry and tropospheric ozone. Atmos Environ 34(12):2131–2159
28. Sye S, Renganathan M (2019) NOx emission control strategies in hydrogen fuelled automobile engines. Aust J Mech Eng. https://doi.org/10.1080/14484846.2019.1668214
29. Pagnin L et al (2021) SO2- and NOx- initiated atmospheric degradation of polymeric films: morphological and chemical changes, influence of relative humidity and inorganic pigments. Microchem J 164:106087
30. Middleton J et al (2013) The effect of ozone and high temperature on polymer degradation in polymer core composite conductors. Polym Degrad Stab 98(11):2282–2290
31. Hoffmann A, Grossmann J, Zellner R (2005) Direct measurements of the OH and NO2 evolutions in pulsed photo-oxidation studies of hydrocarbons: A method to quantify detailed and integral oxidation mechanisms in NOx containing air. J Photochem Photobiol, A 176(1):260–269
32. Getlichermann M, Daro A, David C (1994) Degradation of polymer blends: Part VII. Photo-oxidation in natural weathering conditions of polyethylene containing styrene-butadiene or styrene-isoprene copolymers. Polym Degrad Stab 43(3):343–352
33. Soenen H et al (2021) Rheological and chemical properties of field aged binders and their variation within the wearing course. Road Mater Pavement Des. https://doi.org/10.1080/14680629.2021.1994450
34. Masson J-F et al (2011) 10-Natural weathering of styrene–butadiene modified bitumen. Polymer Modified Bitumen. Elsevier, pp 298–335
35. Hofko B et al (2020) Bitumen ageing–Impact of reactive oxygen species. Case Stud Construct Mater 13:e00390
36. Mirwald J et al (2020) Understanding bitumen ageing by investigation of its polarity fractions. Construct Build Mater. https://doi.org/10.1016/j.conbuildmat.2020.118809
37. Mirwald J et al (2020) Investigating bitumen long-term-ageing in the laboratory by spectroscopic analysis of the SARA fractions. Construct Build Mater. https://doi.org/10.1016/j.conbuildmat.2020.119577
38. Mirwald J et al (2020) Impact of reactive oxygen species on bitumen aging - The Viennese binder aging method. Construct Build Mater. https://doi.org/10.1016/j.conbuildmat.2020.119495
39. Steiner D et al (2016) Towards an optimised lab procedure for long-term oxidative ageing of asphalt mix specimen. Int J Pavement Eng 17(6):471–477
40. Maschauer D et al (2018) Viennese aging procedure – Behavior of various bitumen provenances. In: Poulikakos L et al (eds) RILEM 252-CMB Symposium - Chemo-Mechanical Characterization of Bituminous Materials. Springer Nature, Switzerland, pp 62–67
41. Österreich R (1992) Bundesgesetz für die Republik Österreich: 210. Bundesgesetz: Ozongesetz. Republik Österreich, Vienna
42. Österreich R (2022) Gesamte Rechtsvorschrift für Immissionsschutzgesetz – Luft. Republik Österreich, Vienna
43. CEN (2012) EN 14770: Bitumen and bituminous binders - Determination of complex shear modulus and phase angle - Dynamic Shear Rheometer (DSR). Brussels
44. Johnston HS (1992) Atmospheric ozone. Annu Rev Phys Chem 43(1):1–31
45. Hard T et al (1986) Diurnal cycle of tropospheric OH. Nature 322(6080):617–620
46. Jacquot F et al (2002) Kinetics of the oxidation of carbon black by NO2: Influence of the presence of water and oxygen. Carbon 40(3):335–343
47. Bailey PS (1958) The reactions of ozone with organic compounds. Chem Rev 58(5):925–1010